Analysis of Nonlinear Flow and Heat Transfer Issues in Nanofluid by Using RK-4th Order Method

Mahendra Pratap Pal[1]
Deapartment of Mathematics, Jaypee Institute of Information Technology, Noida, India[1]
Lokendra Kumar[2]
Deapartment of Mathematics, Jaypee Institute of Information Technology, Noida, India[2]

Abstract:- Nanofluids, composed of a base fluid with dispersed nanoparticles, have gained significant attention due to their unique thermal and flow characteristics. Understanding the nonlinear flow and heat transfer phenomena in nanofluids is crucial for optimizing their performance in engineering applications. In this study, we propose using the Runge-Kutta 4th order (RK-4) numerical method to analyze these issues. The RK-4 method is known for its accuracy and efficiency in solving ordinary differential equations. By applying this method to the governing equations of fluid flow and heat transfer, we can accurately capture the nonlinear behavior of nanofluids. We investigate various nonlinear phenomena, such as boundary layer separation, flow instability, and heat transfer enhancement, considering factors like nanoparticle concentration, size, shape, fluid properties, Reynolds number, and temperature gradient. The RK-4 method provides accurate solutions, revealing critical parameters that affect flow and heat transfer behavior. Comparisons with experimental data and other numerical methods validate the approach, demonstrating its reliability. Parametric studies are conducted to optimize nanofluid characteristics for improved heat transfer and fluid flow. This research enhances our understanding of nonlinear flow and heat transfer in nanofluids and enables efficient numerical analysis, opening new avenues for improving nanofluid-based systems.
Keywords: *Nanofluid, nanoparticles, Runge Kutta method, unsteady flow fluid.*

1. Introduction

Nanofluids have a higher convective heat transfer coefficient because solid nanoparticles transfer heat more efficiently than liquid ones [1]. Nanofluids can be used in many ways, from cooling microsystems to converting energy (as the heat volume of base liquid would be replaced along with nano-additives). A natural and practical approach to modifying a working fluid's thermophysical characteristics and heat transfer rate includes suspending nano-sized solid particles (metal or nonmetal) in a warmed or cooled working fluid [2]. The result is a nanofluid that has a greater thermal conductivity than the base fluid when a base fluid is mixed with nanosized particles. Heat transfer rates can be improved by employing nanofluid due to its more difficult thermal conductivity than the base fluid.

The concept of mixing nonmetallic or metallic particles into a conventional fluid such as mineral, water, oils, or ethylene glycol to increase its heat transfer properties is conceived which is considering that solids have greater thermal conductivity than liquids. Nanoscale particles have attracted more consideration than other particle sizes, including micro and Nanoscale particles because of different difficulties in reducing pressure loss across the system or preserving the homogeneity of the mixture [3].

1.1. Nonlinear Problems of Flow in Nanofluids

One of the more well-known difficulties in fluid mechanics is the movement of fluid over a revolving disc, which can be used in both theories and practice in engineering and science. Research into flow over a rotating disc has been extensive and this type of flow has several practical applications in spaces including computer caches, medical kits, rotating machinery, and electrical tools [4].

Nanofluids have been successfully used in a range of sectors and applications, including microchannel cooling, heat recovery, and underfloor heating methods. The notion of incorporating metallic or nonmetallic particles into a common fluid such as liquid, mineral oils, or ethylene glycol to increase heat transfer capabilities originated because of this property solids have greater thermal conductivity than liquids [3]. Since the heat transfer channel and the heat transfer plane have different thermal conductivities, this impacts the heat transfer constant at the middle of the channel or the heat transfer plane. It has a broad variety of uses in metallurgy and chemical engineering, notably in polymer extrusion and metallic plate cooling. It is also used in paper film drawing, glass blowing, and manufacturing [5]. Nanofluid transport must be studied using the continuum and mean-field concepts if individual molecules are cleanly separated at the Nanoscale [6]. The analysis of nonlinear flow in nanofluids involves investigating the behavior of nanofluid flow under the influence of external forces, such as pressure gradients, magnetic fields, or centrifugal forces. These forces can induce complex flow patterns, including laminar, transitional, and turbulent flows, and can have a major effect on nanofluids' efficiency as a convective heat sink. The Navier-Stokes and other governing equations for fluid flow can be quantitatively solved using the RK-4 method, while considering the properties of the nanoparticles and their interactions with the bulk fluid.

Furthermore, studying heat transfer in nanofluids requires examining the thermal conductivity enhancement resulting from the presence of nanoparticles. The thermal behavior of nanofluids is influenced by factors like nanoparticle concentration, material properties, and size. Heat transfer mechanisms, such as conduction, radiation, and convection, play vital roles in determining the overall heat transfer characteristics of nanofluids. Through the application of the RK-4 method, we aim to model and analyze the nonlinear heat transfer processes in nanofluids, considering the intricacies associated with the particle-fluid interactions.

1.2. Nanoparticles in Nanofluids

According to the findings of some investigation’s nano particles in suspension and the thermal and concrete characteristics of the ground fluid have a major effect on the density, thickness, and thermal conductivity of nanofluids. It is the shape and size of the nanoparticles, as well as their volume fraction, that determine the enhanced properties of nanofluids. Other factors that influence these enhanced properties include the grouping of the fluid particle around the solid nanoparticle, as well as the axial orbit of the nanoparticles that are suspended in the air [7].

1.3. Effects of a Magnetic Field on Nanofluids

Glass fiber hot rolling and melt-pinning, as well as rubber and plastics exclusion, are some of the applications of this technology. Metal nanoparticles can be added to a liquid to boost its heat conductivity.

Recently, several researchers have turned to nanofluids to aid with sheet-stretching issues. Flowing boundary layer nanofluids of a stretched sheet revealed heat transfer phenomena while the surface temperature stayed constant. There is a fixed value, and it is represented by the coordinate surface as seen in Fig. 1 [8].

The ability to change thermal conductivity in response to temperature is crucial in many fields, including engineering, space technology, and communications. In general, as the temperature ratio parameter is increased, the Nusselt number of a non-Newtonian fluid also increases [9]. Radiative heat transfer is an essential concept to grasp since it is applied in a variety of settings, including nuclear reactor cooling, combustion, and power generation. Solar radiation processes involving cognitive thinking are essential for the development of novel energy conversion systems, such as those that operate at higher temperatures. Astrophysical fluxes, solar power technologies, spaceship re-entry, and other sources of energy, such systems must be constructed using fossil fuel combustion [10].

Nanoparticles improved the performance of a thermal system. However, the deposition and aggregation of nanofluids inhibited heat transmission during operation. Several approaches have been suggested in the open paper to circumvent the accumulating characteristics of the material. One of the most effective and extensively utilized methods is ultrasonic vibration. An experimental investigation was carried out in a procedure to control the effect of ultrasonic waves on thermal conduction and compression drop component of intake turbulent flow [11].

This paper is arranged in the following section Part 1 is an introduction; Part 2 is the literature review; Part 3 is an overview of the context for the work; Part 4 is a discussion of the research issue statement; and Part 5 is the research technique, the section 6 contains a numerical method to solve differential equations, section 7 contains the results and discussion part while the last section contains the conclusion of the paper.

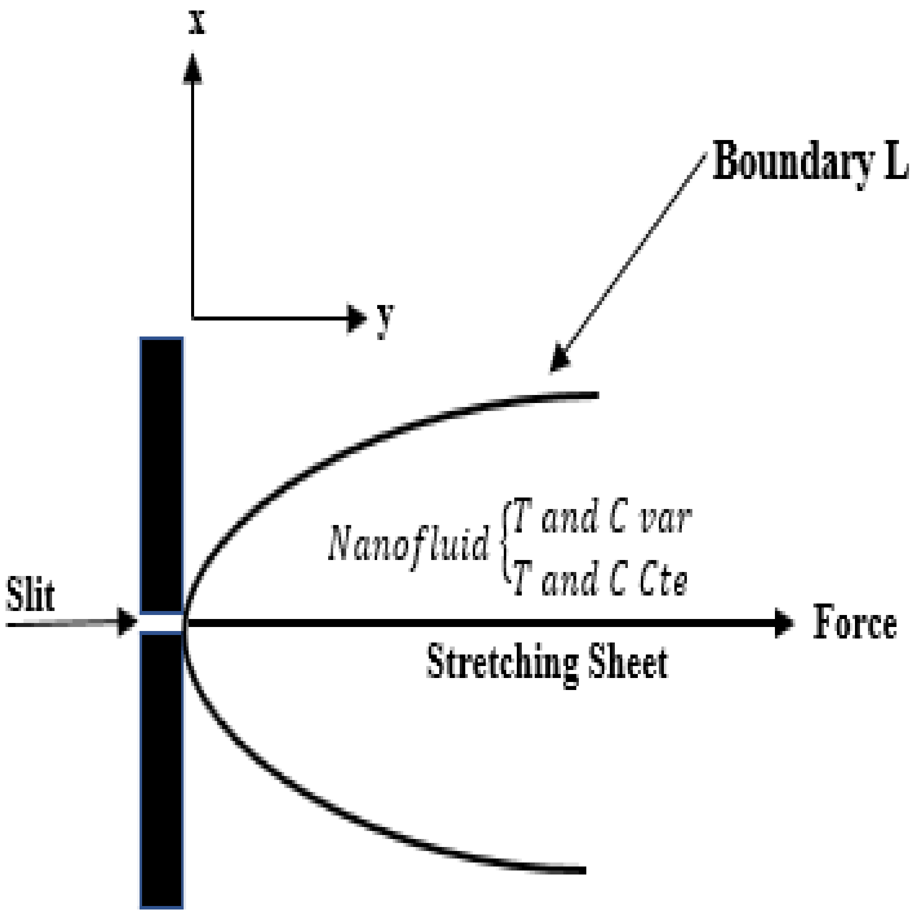

Fig. 1. A visible problem model and the corresponding coordinate system [8].

2. Review of Literature

The following study expands the numerical method of various nonlinear flow boiling heat transfer issues in nanofluids. Several researchers explained their findings as seen below.

Loganathan et. al., (2022) [12] suggested that Williamson nanofluid's radiation effects on a semi-infinite vertical plate and how they change depending on the values of the controlling parameters. Experiments were conducted on a variety of nanofluids to learn more about the ways in which their fluidity altered over time. A handful of the more important results are as follows: Acceleration decays as a function of the Weissenberg number and the radiation parameter. Cu-water Based on these velocity profile graphs, Williamson nanofluid seems to be the fastest. Both Ag and Al2O3 nanofluid profiles show localized regions of highest and lowest skin friction. As can be seen from the data above, Williamson nanofluids behave quite differently from Newtonian fluids.

Siddique et al., (2022) [13] intended magnetohydrodynamics (MHD) across an exponentially expanding surface, with a special emphasis on Dufour and Soret effects involving a second order nanofluid. Mixed convection effects and thermal conductivity are studied to shed light on the heat transfer mechanism. The subsequent issues were resolved using a computer technique called Homotropy analysis (HAM). The graphs and charts below illustrate the ways in which environmental influences alter concentration, temperature, and velocity distributions. There was a lot of agreement between the present findings and the previous research. It is more reasonable to assume a flow with varying thermal conductivity than one with fixed values. Thermophoresis motion, buoyancy ratio, and Brownian motion all contributed to the total rise in fluid temperature. Several very viscous flows are seen in the chemical and mechanical industries; these findings suggest that the porous, slippery surface may be advantageous in these fields.

Uddin et al., (2021) [7] utilized the Runge-Kutta technique and a hybrid shooting strategy based on Particle Swarm Optimization are to solve the resultant equations. Models of viscosity and thermal conductivity that take into consideration nanoparticle size, concentration, and shape are used to better understand the natural and thermal properties associated with Nanofluids.

Kumar et al., (2021) [11] calculated that the tests are solved using computational fluid dynamics (CFD). There has been a major increase in both the heat transfer constant as well as the friction aspect of the nanofluid flow heat exchanger tube. The investigation of twisted tape characteristics was carried out using a SiO2 = H2O nanofluid as the medium for Reynolds numbers feeding on 5000 to 17,000, and the impact was published.

Daniel et al., (2020) [10] studied that The Keller box approach is then utilized to numerically solve the changed equations systems. Several important parameters, including temperature, acceleration, absorption, Nusselt as well as skin friction, are explored in-depth. The data obtained has been subjected to a validation procedure.

Chitsazan et al., (2018) [2] provided a comprehensive analysis of numerically solving a system of nonlinear coupled differential equations. The study utilized the fourth order Runge-Kutta method as a numerical technique to address the challenges posed by binary nonlinear ordinary differential equations. The study further investigated the effect of several characteristics on temperature and velocity distributions, such as Eckert number, Magnetic parameter, and others, was examined.

Daniel et al., (2018) [6] suggested that the electrical Magneto hydrodynamic (MHD) nanofluid model must consider Brownian motion, thermophoresis, thermal radiation, viscosity dissipation, and Joule heat generation. A wide variety of emergent factors must be used to numerically solve the barrier layer equations as a set of non-similar parabolic calculations using the Keller box numerical approach.

Yin et al., (2017) [4] estimated that using Von Karman transformations, nonlinear governing equations must be transformed into ordinary differential calculations. The homotopy analysis method (HAM) has been utilized for these ordinary differential equations to solve them. It would be demonstrated and thoroughly investigated how changes in the stretching power constant, solid fig. percent, and the form of Nanofluids affect acceleration and temperature fields.

Salari et al., (2014) [8] computed that the use of a laminar nanofluid flow to transport heat over a stretched flat sheet is shown. As a result, it is necessary to consider two different groups of boundary conditions (BCs). There are two approaches to solving this barrier value problem: one is to convert the governing equations into a barrier value problem in comparison fluid, and the other is to numerically solve the new set of equations for the continuous (Case 1) or the lined streamwise deviation the relationship between the nanoparticle’s capacity fraction as well as the wall temperatures (Case 2), respectively.

Ahmadi et al., (2014) [3] calculated that the unsteady movement of a nanofluid and the associated heat transfer generated was investigated by linear movement of an unbowed plane of metal, and the velocity profile has been raised by increasing the steadiness parameter. Furthermore, raising them has resulted in a significant increase in the temperature profile, suggesting that heat transfer capabilities must be improved by choosing optimal nanoparticle sizes.

Noghrehabadi et al., (2012) [5] calculated the use of numerical methods to explain the resultant differential equations. The velocity slip factor was shown to reduce and improve momentum boundary layer thickness and thermal boundary layer thickness. Reduced slip parameter has a significant impact on the Nusselt as well as decreased Sherwood number, as well as the rate of flow as well as surface shear on the stretched sheet, among other things There is a wide range of authors who used the technique and presented their discoveries, as can be seen in table 1.

Table 1

Summarize the table of compared reviewed literature.

Author Name	Technique	Outcomes	Research Gap

LOGANATHAN, et. al., (2022) [12]	Williamson nanofluid	The velocity profiles demonstrate that the Williamson nanofluid composed of Cu water has the maximum velocity. Nanofluidic profiles of Ag and Al2O3 show maximum and minimum values for local skin friction.	Future research is sure to uncover novel ways in which these studies might be applied to pressing societal issues. In addition, the present research incorporated both transitional and turbulent flows and different geometries.
Siddique et al., (2022) [13]	MHD	Based on the specifics of the findings, the porous, slippery surface may have applications in the chemical and mechanical industries. for controlling various very viscous flows.	All information in this document has been carefully researched and is believed to be accurate; however, this is the first study outline to examine, generated by an exponentially permeable stretched sheet with varying thermal conductivity, a second-class nanofluid experiences unstable slip and MHD nonlinear radiative flow.
Uddin et al., (2021) [7]	Hybrid shooting	The stable and realistically feasible solutions are selected out of the captured dual solutions with the aid of calculated eigenvalues.	The scientists want to improve the findings in the future by adjusting the stretching velocity parameter to increase faster convection and lessen the skin's resistance to heat flow.
Kumar et al., (2021) [11]	CFD	It is discovered that providing twisted the use of tape increases the assessment of heat transfer and the calculation of friction in the SiO_2/H_2O Fluid flow heating exchange tube.	In future research, authors will work on the same technique to increase the assessment of heat transfer in nanofluid.
Daniel et al., (2020) [10]	Keller Box Method.	Considering heat convection given to both radiation and convection.	Thermal emission, viscous dissipation, Ohmic heating, and chemical reaction have all been used passively to study the natural convection of nanofluid which is future work of the previous study.
Chitsazan et al., (2018) [2]	Runge - Kutta	It was possible to get an explanation for the linked nonlinear ordinary differential equations by using a numerical approach.	The existence of viscous dissipation effects must be because of the temperature rising.
Daniel et al., (2018) [6]	Kelle Box.	According to this research's findings, which were based on an implicit finite difference scheme, the findings match those of a prior study in a very restricted way.	Heat and mass transport are two problems that were mentioned in the previous work that need to be addressed in an electrically controlling nanofluid movement that is exacerbated when sheets are stretched or shrunk. These problems are resolved in the work.

Yin et al, (2017) [4]	HAM	Radial and axial acceleration are increased by stretching strength, it reduces skin friction, local Nusselt number, and tangential momentum; nevertheless, it also reduces thermal barrier layer thickness and width of the heat barrier layer.	Effect of nanofluid volume percentage and type on acceleration and temperature.
Salari et al., (2014) [8]	Numerical Solution (Non-Linear Differential equation)	The BCs in Case 2 have a lower Nusselt number and a lower Sherwood number in comparison to Case 1.	The nanofluid flowing through a stretching sheet with linear changes in both parameters across the surface is a problem which are not done in previous study. In the work research are solved this.
Ahmadi et al., (2014) [3]	Differential Transformation Method	Enlarging the S parameter increases the velocity profile. Furthermore, raising them has resulted in a significant increase in the temperature profile, suggesting that heat transfer capabilities must be improved by choosing optimal nanoparticle sizes.	Graphically, the important mistakes of the produced solutions in previous work have been represented and correct them in the work.
Noghrehabadi et al., (2012) [5]	MWCNTs-COOH and Ag nanoparticle	Based on the thermal conductivity ratio, it was discovered that the hybrid nanofluid had a 47.3% increase in thermal conductivity.	Finally, hybrid nanofluids are the nanofluids of the future in heat transfer applications.

3. Background Study

Nanofluids are studied as they travel over and transfer heat from a spinning disc at a constant stretching rate. Cu, Al2O3, and CuO are the three types of nanoparticles that are considered when using water-based nanofluids: Cu, Al2O3, and CuO. The problem of fluid movement over a revolving disc is a classic problem that has both theoretical and practical applications in the field of fluid mechanics. The Von Karman transformation is applied as part of the RK-4, which is utilized to resolve the simplified governing calculations. Consequently, the radial and axial velocities improve while the tangential velocities or width of the thermal boundary sheet fall as the stretching strength limitation, skin friction, as well as the Nusselt Number growth, respectively. The effects of size fraction and nanofluid kinds on the speed and temperature fields are investigated in greater depth [4].

4. Problem Formulation

The heat transfer of a laminar nanofluid flow over a revolving disc on a piece of paper is numerically observed. The flow and heat communication of nanofluids over revolving discs are examined in the proposed study using various nanoparticles. This classic fluid mechanics problem involves fluid flow across a rotating disc, which has both theoretical and practical values. An incompressible 3D revolving flow of viscous fluid among infinite walls was studied and the convective flow was attributed to resistance power due to heat and molecular transmission. The Runge Kutta Method and non-linear partial differential equation are the first two techniques employed in this problem.

5. Research Methodology

This section provides the proposed methodology of the research work. The methods used in this study to handle the issue of steady and erratic heat transfer in nanofluid flow are described in further detail below. The Runge-Kutta technique is used to numerically solve the unsteadiness of nanofluid heat transfer utilizing the boundary conditions of a nonlinear differential equation with unsteadiness. The mathematical approach was used to resolve them when the numerical solution resulted in the emergence of linked nonlinear differential equations.

5.1. *Heat transfer in Steady nanofluid flow*

The problem of fluid flow across a revolving disc is a classic fluid mechanics problem with both theoretical and practical applications. This flow across rotating disc research has been carried out in theoretical disciplines for a variety of practical purposes, such as computer cache devices, electrical devices, revolving machinery, and medical equipment.

5.2. *Problem Dynamics*

This study investigates the movement and heat transmission of nanofluid over a stretching revolving disc using 3 kinds of nanoparticles: CuO, Cu, Al2O3, and Cu. Consider the flow of an incompressible, stable, and axially symmetric nanofluid across a revolving disc at z = 0 rotating at an angular acceleration Ω of the disc stretched in the radial direction r at a constant rate s. Fig. 2 depicts a physical model of a revolving disc.

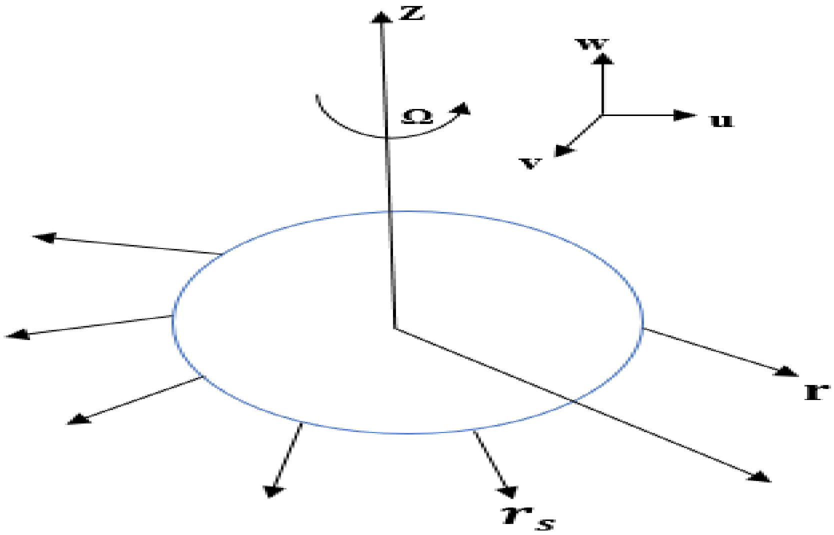

Fig. 2. Physical Model of Rotating Disk [4].

$$\frac{\partial u}{\partial r}+\frac{u}{r}+\frac{\partial \omega}{\partial z}=0 \tag{1}$$

$$u\,\frac{\partial u}{\partial r}-\frac{v^2}{r}+w\frac{\partial u}{\partial z}+\frac{1}{p_{nf}}\frac{\partial p}{\partial r}=\frac{\mu_{nf}}{\rho_{nf}}\left(\frac{\partial^2 u}{\partial r^2}+\frac{1}{r}\;\frac{\partial u}{\partial r}-\frac{u}{r^2}+\frac{\partial^2 u}{\partial z^2}\right) \tag{2}$$

$$u\,\frac{\partial v}{\partial r}+\frac{uv}{r}+w\frac{\partial v}{\partial z}=\frac{\mu_{nf}}{\rho_{nf}}\left(\frac{\partial^2 v}{\partial r^2}+\;\frac{\partial}{\partial r}\left(\frac{v}{r}\right)+\frac{\partial^2 v}{\partial z^2}\right) \tag{3}$$

$$u\,\frac{\partial w}{\partial r}+\frac{uv}{r}+w\frac{\partial v}{\partial z}+\frac{1}{p_{nf}}\frac{\partial p}{\partial z}=\frac{\mu_{nf}}{\rho_{nf}}\left(\frac{\partial^2 w}{\partial r^2}+\frac{1}{r}\;\frac{\partial w}{\partial r}+\frac{\partial^2 w}{\partial z^2}\right) \tag{4}$$

$$u\,\frac{\partial T}{\partial r}+w\,\frac{\partial T}{\partial z}=\alpha_{nf}\left(\frac{\partial^2 T}{\partial r^2}+\frac{1}{r}\frac{\partial T}{\partial r}+\frac{\partial^2 T}{\partial z^2}\right) \tag{5}$$

The boundaries are given below:

$$Z=0:\;\; u=sr,\; v=\Omega r,\; w=0,\; T=T_w \tag{6}$$

$$z\to\infty:\; u\to 0,\; v\to 0,\; T\to\infty,\; P\to\infty \tag{7}$$

Where T is the absolute temperature of a nanofluid in this equation, T_∞ the temperature of the ambient nanofluid, P is pressure, and the rotating nanofluid pressure P1, μ_{nf} and α_{nf} are indeed the nanofluid's effective density with current diffusivity, ρ_{nf} is the viscosity of the nanofluid, which differs from one another.

$$\mu_{nf=}\frac{\mu_f}{1-\varphi)^{2.5}}\alpha nf = \frac{k_{nf}}{(\rho C_\rho)_{nf}}, \ \rho_{nf=(1-\varphi)\rho f+\varphi\rho_S} \tag{8}$$

$$(\rho C_\rho)_{nf} = (1-\varphi)(\rho C_\rho)_f + \varphi(\rho C_\rho)_s, \tag{9}$$

$$\frac{k_{nf}}{k_f} = \frac{(k_{s+2k_f})-2\varphi(k_{f-k_s})}{(k_s+2k_f)+\varphi(k_f-k_s)} \tag{10}$$

φ is the nanoparticle size fraction; the area of φ is 0 to1. ρ_f is the thickness of the fluid fraction, ρ_f and ρ_s are the thicknesses of the fluid and the hard fractions respectively. The nanofluid's heat capacity is known by $(\rho C_\rho)_{nf}$ and k_{nf} is approximating the nanofluid's effective thermal conductivity as given by Oztop's model, nanofluid thermal conductivity cannot be accurately measured using just spherical nanoparticles as a proxy.

Using Roseland approximation for radiation it has

$$q_r = -\frac{4\sigma^*}{3\delta}\frac{\partial T^4}{\partial y} \tag{11}$$

Here σ* and δ are the Stefan–Boltzmann constants as well as the average absorption coefficient are the two quantities to consider. The assumption that temperature fluctuations inside the stream were sufficient for the sake of the discussion small that they do not affect the flow T4. After applying the Taylor series to the problem, it must be written as a linear function T4 regarding the temperature of the streaming site T∞ as well as ignoring higher-order words.

$$T^4 \cong \ 4T_\infty^3 T - 3T_\infty^4 \tag{12}$$

Using (7) and (10) in (3), it has been obtained.

$$u\frac{\partial T}{\partial \varkappa} + v\frac{\partial T}{\partial y} = \alpha\nabla^2\mathrm{T} + \frac{1}{(\rho c)_f}\left(\frac{16\sigma^* T^3{}_\infty}{3\delta}\frac{\partial^2 T}{\partial^2 \varkappa}\right) + \tau\left[D_B\frac{\partial\emptyset}{\partial y}\frac{\partial T}{\partial y} + \left(\frac{D_T}{T_\infty}\right)\left(\frac{\partial T}{\partial y}\right)^2\right] \tag{13}$$

It is necessary to incorporate the appropriate approximate solution to turn into ordinary differential equations.

$$\eta = \frac{y}{x}Ra_x{}^{1/4}, \psi = \alpha Ra_x{}^{\frac{1}{4}}s(\eta), \theta(\eta) = \frac{T-T_\infty}{T_w-T_\infty}, f(n) = \frac{\phi-\phi_\infty}{\phi_w-\phi_\infty} \tag{14}$$

Using the Rayleigh number for the area, which is given as

$$R_{ax} = \frac{(1-\phi_\infty)g\beta(T_w-T_\infty)x^3}{vu} \tag{15}$$

As well as the streaming function (x, y) being specified in such a way that

$$u = \frac{\partial\psi}{\partial y}, v = -\frac{\partial\psi}{\partial x} \tag{16}$$

As a result, the continuity condition is met in the same way. After certain algebraic tinkering, the momentum is restored.

$$s''' + \frac{1}{4\mathrm{Pr}}\left(3s'' - 2s'^2 - 4M\sqrt{Prs'}\right) + \theta - Nrf = 0,$$
(17)

$$\left(1 + \frac{4N}{3}\right)\theta'' + \frac{3}{4}s\theta' + Nbf'\theta' + Nt\theta'^2 = 0, \tag{18}$$

$$f'' + \frac{3}{4}Lesf' + \frac{Nt}{Nb}\theta'' = 0, \tag{19}$$

Where η is the primes signify distinction in relation together with nondimensional characteristics. The following limits are established: The percentage of the nanofluid profile that is solid is defined by the parameter f. The buoyancy-ratio parameter (Nr), the Lewis number (Le), the squeezing parameter (S), ss the magnetic parameter (M), the thermophoresis parameter (Nt), and the radiation parameter (N) are all examples of parameters; likewise, the Brownian motion parameter (Nb) and the Prandtl number (Pr) are examples of parameters.

$$P_r = \frac{v}{\alpha},\ N_r = \frac{(\rho_p = \rho f_\infty)(\phi_w = \phi_\infty)}{\rho f_\infty \beta (T_w - T_\infty)(1-\phi_\infty)},\ N_b = \frac{(\rho_c)_p D_B(\phi_w - \phi_\infty)}{(\rho_c)_f \alpha}, Le = \frac{\alpha}{D_B}\quad N_t = \frac{(\rho_c)_p D_T(T_w - T_\infty)}{(\rho_c)_f \alpha T\infty},$$

$$\mathrm{M} = \frac{\alpha {B_o}^2 x^{1/2}}{\sqrt{(1-\phi_\infty) g\beta (T_w - T_\infty)}}\ \text{and}\ \mathrm{N} = \frac{4\alpha^* T^3{}_\infty}{k\delta}$$

The corresponding boundary conditions are

$$\mathrm{f}(\eta) = 1\quad \mathrm{sr}(\eta) = 0,\ \theta(\eta) = 1,\ \mathrm{s}(\eta) = 0,\ \text{at}\quad \eta = 0 \tag{20}$$

$$\theta(\eta) = 0,\ \mathrm{sr}(\eta) = 0,\ \mathrm{f}(\eta) = 0\text{as}\quad \eta \to \infty \tag{21}$$

The Nusselt number (Nu) is a quantity that is of practical importance as well as the Sherwood number (Sh) defined as follows:

$$N_u = \frac{xq''_w}{k(T_w - T_\infty)} \tag{22}$$

$$Sh = \frac{xq''_w}{D_B(\emptyset_w - \emptyset_\infty)} \tag{23}$$

$$N_{ur} = Rax^{\frac{1}{4}}Nu = -\left(1 + \frac{4N}{3}\right)\theta'(0) \tag{24}$$

$$Shr = Rax^{\frac{1}{4}}Sh = -f'(0) \tag{25}$$

5.3. *Heat Transfer in unsteady nanofluid flow*

The researchers hypothesized that the convective flow was caused by an unstable, incompressible, rotating 3D varied convection flow of sticky fluid among 2 limitless walls. They were able to demonstrate how a magnetic field can alter the flow's temperature and speed using a different magnetic number. Researchers are trying to fig. out an unsteady viscosity nanofluid's heat flow as well as movement patterns movement (graphene oxide in liquid) in a rotating system among two absolute flat plates (the lower one being permeable).

5.3.1 *Problem Dynamics*

Graphene oxide nanoparticles in a magneto-hydrodynamic viscous flow are being investigated in a network with insulated walls and a lower porous wall to better understand the heat transfer and movement field. The permeable bottom wall of the channel is at y = 0 and is expanded beside the x-direction with a speed of $U_w = \frac{ax}{1-ct}$ whilst the upper wall is at $h(t) = \sqrt{\frac{v(1-ct)}{a}}$. The temperature of the channel's lower wall (T_w) is considered to remain constant, whereas the temperature of the channel's squeezing wall (T_h) is greater one, where $(T_w > T_h)$.

Fig. 3 illustrates a geometric scenario involving the flow and heat transmission of a viscous and unstable nanofluid, specifically graphene oxide in water. This occurs within the confined space between two horizontally oriented plates, with one plate being permeable, in a revolving framework.

The following are the flow and heat transfer equations that apply to this rotating system:

$$\frac{\partial u}{\partial x} + \frac{\partial v}{\partial y} = 0 \tag{26}$$

$$\frac{\partial u}{\partial t} + u\frac{\partial u}{\partial x} + v\frac{\partial u}{\partial y} + 2\frac{\omega_0}{1-ct}w = -\frac{1}{\rho_{nf}}\frac{\partial P}{\partial x} + v_{nf}\left(\frac{\partial^2 u}{\partial x^2} + \frac{\partial^2 u}{\partial y^2}\right) - \frac{\sigma B^2}{\rho_{nf}(1-ct)}u \tag{27}$$

$$\frac{\partial v}{\partial t} + u\frac{\partial v}{\partial x} + v\frac{\partial v}{\partial y} = -\frac{1}{\rho_{nf}}\frac{\partial P}{\partial x} + v_{nf}\left(\frac{\partial^2 v}{\partial x^2} + \frac{\partial^2 v}{\partial y^2}\right) \tag{28}$$

$$\frac{\partial w}{\partial t} + u\frac{\partial w}{\partial x} + v\frac{\partial w}{\partial y} - 2\frac{\omega_0}{1-ct}u = v_{nf}\left(\frac{\partial^2 w}{\partial x^2} + \frac{\partial^2 w}{\partial y^2}\right) - \frac{\sigma B^2}{\rho_{nf}(1-ct)} \tag{29}$$

$$\frac{\partial T}{\partial t} + u\frac{\partial T}{\partial x} + v\frac{\partial T}{\partial y} = \frac{k_{nf}}{(\rho c_p)_{nf}}\left(\frac{\partial^2 T}{\partial x^2} + \frac{\partial^2 T}{\partial y^2}\right) + \frac{\mu_{nf}}{(\rho c_p)_{nf}}\left[4\left(\frac{\partial u}{\partial x}\right)^2 + |\left(\frac{\partial u}{\partial x} + \frac{\partial v}{\partial x}\right)^2 + \left(\frac{\partial w}{\partial x}\right)^2 + \left(\frac{\partial w}{\partial y}\right)^2\right] \tag{30}$$

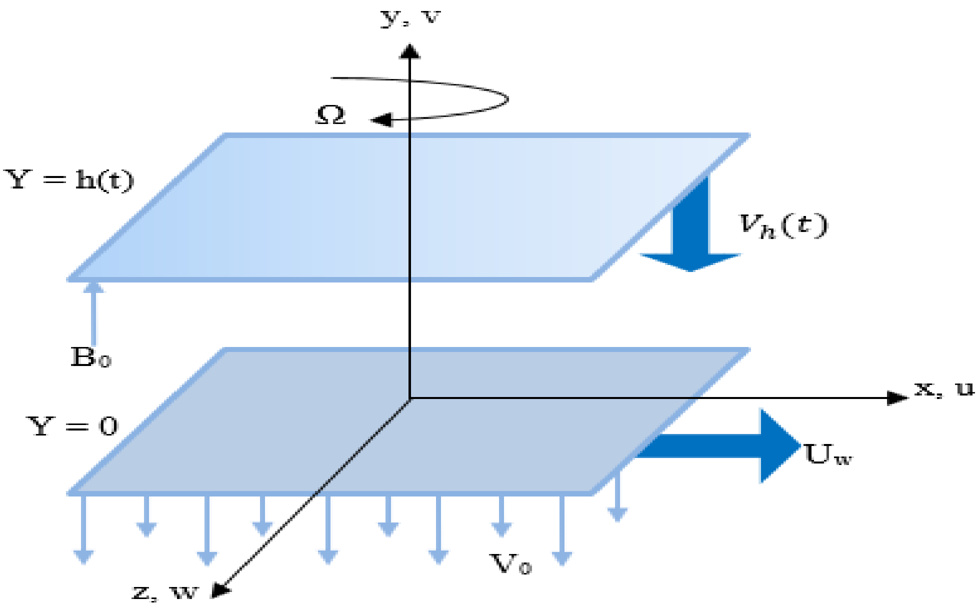

Fig. 3. Problem of Geometry [2].

This problem's relevant boundary situations are:

At y = 0: u (x, y, t) = Uw = $\frac{ax}{1-ct}$, v(x,y,t)= , $w\,(x, y, t) = 0, T(x, y, t) = T_{w,}$ (31)

At y = h(t): u (x, y, t) = 0, v(x,y,t)= $-\frac{c}{2}\sqrt{\frac{v}{a(1-ct)}}$, $w(x, y, t) = 0, T(x, y, t) = T_h$ (32)

The stretching rate of the bottom wall is greater than zero in the above calculations. w, v, and u represent the independent mechanisms responsible for generating velocity in the z, y, and x axes. T signifies temperature, k_{nf} denotes the actual thermal conductivity of nanofluid, ρ_{nf} denotes current thickness, and μ_{nf} denotes current dynamic thickness.

The lower wall stretching rate is represented by a > 0 in the preceding equations. In the x, y, and z dimensions, these vectors represent the velocity components u, v, and w. P represents pressure, B0 represents the necessary external magnetic field, T represents temperature, knf stands for effective thermal conductivity of nanofluid, and ρnf represents effective density. Additionally, μnf denotes the effective dynamic viscosity, while the remaining three factors (effective density, effective thermal conductivity and effective dynamic viscosity) are explicitly specifsied.

$$\rho_{\eta f} = \rho_f(1-\emptyset) + \rho_s\emptyset_s \tag{33}$$

$$(\rho C_p) = (\rho C_p)_f(1-\emptyset) + (\rho C_p)_s \tag{34}$$

$$\mu_{nf} = \frac{\mu_f}{(1-\emptyset)^{2.5}} \tag{35}$$

$$\frac{k_{ns}}{k_f} = \frac{k_s+2k_f-2\emptyset(k_f-k_s)}{k_s+2k_f+2\emptyset(k_f-k_s)} \tag{36}$$

$$\nu_{\eta f} = \frac{\mu_{nf}}{\rho_{nf}} \tag{37}$$

In addition, in these relationships σ is a measure of the fluid's conductivity, ϕ is the proportion of nanoparticles in their total volume, υnf is the fluid density of a fluid α. The thermal diffusivity of a nanofluid is defined as Cp as well as subscripts are the specific heat produced by a fluid at a pressure f and s Both the base fluid, as well as the solid nanoparticles, relate to each other. The following parameters must be included in the governing equations to make them easier to understand:

$$\eta = \frac{y}{[(1-at)^{1/2}]}, u = \frac{ax}{[2(1-at)]}f'(\eta), v = \frac{a}{[2(1-at)^{1/2}]}f'(\eta), \tag{38}$$

$$w = U_w g(\eta), \theta = \frac{T-T_w}{T_w-T_h}, A = (1-\emptyset) + \emptyset\frac{p_s}{p_f}, \tag{39}$$

$$B = (1-\emptyset) + \frac{(\rho C_p)_s}{(\rho C_p)_f}, C = \frac{k_{nf}}{k_f} \tag{40}$$

By reducing the pressure difference from Equation (41–44), the resulting coupled nonlinear dynamic equations would be generated:

$$f^{IV} - A(1-\emptyset)^{2.5}\left(f'f\text{+f'} - \frac{s_q}{2}(3f\text{+ηf'})\right) - 2\Omega g' - M^2 f" = 0 \tag{41}$$

$$g" + A(1-\emptyset)^{2.5}\left(fg' - f'g - s_q\left(g + \frac{\eta}{2}g'\right)\right) + 2\Omega f' - M^2 G = 0 \tag{42}$$

$$\theta'' + P_r\left(\frac{B}{C}\right)\left(f\theta' - \frac{s_q}{2}\eta\theta'\right) + \frac{P_r}{C(1-\emptyset)^{2.5}}\left[E_c(4f' + g^2) + E_{c_x}(f'^2 + g'^2)\right] = 0 \tag{43}$$

Where the boundary conditions are

$$f(0) = w_o, f'(0) = 1, g(0) = 0, \theta(0) = 1,$$

$$f(1) = \frac{S_q}{2}, f'(1) = 0, g(1) = 0, \theta(1) = 0 \tag{44}$$

The non-dimensional variables are examined in this work.:

Suction parameter (w0) = $\frac{V_o}{ah}$;

The rotation parameter (Ω)= $\frac{w_o}{a}$;

squeezing parameter (Sq) = $\frac{c}{a}$;

Prandtl number (Pr) = $\left(\frac{\mu_{cp}}{k}\right)_{nf}$;

Local Eckert number (ECx) = $\frac{U^2{}_w}{(C_p)_{nf(T_w - T_h)}}$;

magnetic parameter (M)= $\sqrt{\frac{\sigma\beta^2{}_o}{\rho\alpha}}$; and the

Eckert number (Ec) =$\frac{\nu^2}{C_p(T_w - T_h)}$.

The RK-4 order method was chosen in this work to resolve the boundary value issue calculations because it is a convenient approach. Midpoint-based approaches are appropriate for issues with endpoint individualities. Additionally, the fourth order RK technique is a middle-ground process. The RK-4 technique can be used to write the following:

$$y_{i+1} = y_i \frac{1}{6}(k_1 + 2k_2 + 2k_3 + k_4) \tag{45}$$

$$k_1 = E(x_i, y_{i)} \tag{46}$$

$$k_2 = E(x_i + \frac{1}{2}h, y_i + \frac{1}{2}k_1 h \tag{47}$$

$$k_3 = E(x_i + \frac{1}{2}h, y_i + \frac{1}{2}k_2 h \tag{48}$$

$$k_4 = E(x_i + h, y_i + k_3 h) \tag{49}$$

Here, h represents the step size, and y' = E. (x, y) in numerical calculations. RK-4 order method was used to solve nonlinear boundary value problems using the Reconstruction of Variational Iteration Technique) RVIM was used to validate numerical results.

In the analysis of nonlinear flow and heat transport phenomena in nanofluids, the implementation of the fourth order Runge-Kutta (RK-4) approach has proven to be effective. This numerical method is employed to provide an approximate solution for a set of ordinary differential equations (ODEs) that describe the processes of flow and heat transport in nanofluids. By utilizing this approach, researchers can gain insight into the behavior and dynamics of these complex systems. A more detailed explanation of the methodology used can be provided by describing it in the context of ODEs.

Suppose an ODE that represents the heat transfer and nonlinear flows in a nanofluid system. The general form of this ODE can be written as:

du/dt = f(t, u)

where u is the vector of dependent variables, t is the independent variable (time), and f(t, u) represents the nonlinear functions that describe the flow and heat transfer phenomena.

To apply the RK-4 method, we follow these steps:

Step 1: Initialization

Set the initial condition for u, i.e., $u(t_0) = u_0$, where t_0 is the initial time and u_0 is the initial value of u.

Set the step size, Δt, which determines the time interval between successive calculations.

Step 2: Iterative Calculation

Start a loop that iterates from t_0 to t_n, where t_n is the final time.

At each iteration, calculate the intermediate values of u using the RK-4 method.

Step 3: RK-4 Method

Calculate the intermediate values of k_1, k_2, k_3, and k_4 using the following equations:

$$K_1 = \Delta t \times f(t, u)$$

$$K_2 = \Delta t \times f(t + \frac{\Delta t}{2}, u + \frac{K1}{2})$$

$$K_3 = \Delta t \times f(t + \frac{\Delta t}{2}, u + \frac{K2}{2})$$

$$K_4 = \Delta t \times f(t + \Delta t, u + k_3)$$

Update the value of u using the weighted average of these intermediate values:

$u = u + (k_1 + 2k_2 + 2k_3 + k_4)/6$

Step 4: Increment Time

Update the value of t to t + Δt.

Step 5: Termination

Repeat steps 2 to 4 until t reaches the final time t_n.

By following these steps, the RK-4 method iteratively approximates the solution of the ODE describing the heat transfer and nonlinear flow issues in nanofluids. The accuracy of the solution depends on the chosen step size Δt, , often more accurate findings can be obtained with lower step sizes, but at the expense of greater processing time.

The RK-4th order technique is useful for assessing nonlinear flow and heat transfer problems in nanofluids, but its assumptions can have a significant impact on a wide range of parameterss. The considerations are:

Incompressible Flow: The assumption of incompressible flow might be applicable in this analysis if the density changes in the nanofluid due to the presence of nanoparticles are negligible. If the density changes significantly, the incompressible flow assumption may lead to inaccurate results.

Steady-State Flow: The assumption of steady-state flow may be appropriate for this analysis if the flow and temperature fields in the nanofluid remain relatively constant with time. However, if the flow is unsteady or transient, such as in the case of highly time-dependent heat transfer phenomena, the assumption of steady-state flow may not be valid.

Newtonian Fluid: The assumption of a Newtonian nanofluid implies that the viscosity of the nanofluid remains constant regardless of the shear rate or temperature. If the nanofluid exhibits non-Newtonian behavior due to the presence of nanoparticles, this assumption may not accurately illustrate the heat transport and fluid dynamics

Laminar Flow: The assumption of laminar flow may be suitable for this analysis if the flow in the nanofluid remains smooth and well-ordered, with minimal turbulence effects. However, if the flow becomes turbulent due to high velocities or the presence of nanoparticles, the assumption of laminar flow may not capture the actual flow behavior accurately.

Negligible Viscous Effects: Depending on the specific conditions of the nanofluid flow, the assumption of negligible viscous effects may or may not be valid. If the nanofluid has a low viscosity or the flow velocities are high, neglecting viscous effects may introduce significant errors in the analysis. It is important to assess whether viscous effects play a significant role in the nanofluid flow and heat transfer phenomena.

One-Dimensional Flow: It is possible that problems with nonlinear flow and heat transport in nanofluids cannot be properly analyzed using a one-dimensional flow assumption, as the flow behavior in nanofluids can exhibit complex three-dimensional characteristics. Considering the flow as one-dimensional may oversimplify the actual flow field and lead to inaccuracies in the results.

6. A numerical method for the solution

The boundary conditions and the nonlinear coupled differential equations (50)– (52) constitute two-point boundary value problems that are handled by utilizing Runge–Kutta integration of fourth order in the paper. The boundary conditions were listed in the next section,

$$\mathbf{u = 0, T =} \boldsymbol{T_w} \ \emptyset = \emptyset_w, \mathbf{v = 0}, \quad \mathbf{at\ y = 0}$$

$$\mathbf{u} = \boldsymbol{v} = \mathbf{0}, \emptyset = \emptyset_{\infty}, \mathbf{T} \to \boldsymbol{T_\infty}, \quad \mathbf{as} \quad \mathbf{y} \to \infty$$

$$\boldsymbol{s''' + \frac{1}{4\mathrm{Pr}}\left(3s'' - 2s'^2 - 4M\sqrt{Prs'}\right) + \theta - Nrf = 0,} \tag{50}$$

$$\left(1 + \frac{4N}{3}\right)\theta'' + \frac{3}{4}s\theta' + Nbf'\theta' + Nt\theta'^2 = 0, \tag{51}$$

$$f'' + \frac{3}{4}Lesf' + \frac{Nt}{Nb}\theta'' = 0, \tag{52}$$

Where η is the primes signify distinction in relation together with nondimensional characteristics. The following parameters are defined: (Nr) signifies the buoyancy-ratio parameter, (Nb) denote the Brownian motion parameter, (Le) represents the Lewis number, (Nt) denotes the thermophoresis parameter, (M) is the magnetic parameter, S is squeezing parameter, as well as N is the radiation parameter, and (Pr) is a Prandtl number others. θ is dimensionless temperature f representing stream function.

It is an initial value puzzle and necessary to choose a suitable maximum or minimum for the variable in the procedure $\eta \to \infty$, say $\eta\infty$. It has established the first-order system as follows:

$$y_1' = y_2 \tag{53}$$
$$y_1' = y_2 \tag{54}$$
$$y_2' = y_3 \tag{55}$$
$$y_2' = y_3 \tag{56}$$
$$y_3' = -\frac{1}{4Pr}(3y_1y_3 - 2y_2^2 - 4M\sqrt{Pr}y_2) - y_4 + N_r y_6 \tag{57}$$
$$y_4' = y_5 \tag{58}$$
$$y_5' = \left(\frac{-3}{4}y_1y_5 - N_b y_7 y_5 - N_t y_5^2\right)\left(\frac{3}{3+4N}\right) \tag{59}$$
$$y_6' = y_7 \tag{60}$$
$$y_7' = \frac{-3}{4}L_e y_1 y_7 - \frac{N_t}{N_b}y_5' \tag{61}$$

following boundary conditions,

$$y_1(0) = 0, y_2(0) = 0, y_4(0) = 1 \text{ and } y_6(0) = 1 \tag{62}$$

Solve (58) using (62), it must first obtain the values of variables to resolve the boundary value problem $y_3(0)$ i.e., $s''(0), y_5(0)$ i.e., $\theta'(0)$ and $y_7(0)$ i.e.,$f'(0)$ however, no values are provided. The earliest best-guess estimates for $s''(0), \theta'(0)$ and $f'(0)$. It is decided on which variables to use, and the Runge–Kutta integration technique of fourth order is used to get the answer. Then, a comparison between the computed values of $s'(\eta), \theta(\eta)$ and $f(\eta)$ at $\eta\infty$ the given boundary conditions $s'(\eta_\infty) = 0, \theta(\eta_\infty) = 0$ and $f(\eta_\infty) = 0$ and adjust the values of $s''(0), \theta'(0)$ and$f'(0)$. After then, the procedure is repeated until the findings are accurate up to the necessary level of precision 10^{-8} level, following the convergence condition. Fig. 4 depicts the impact of the Prandtl number on $s'(\eta), \theta(\eta)$, and $f(\eta)$.

Fig. 4. (a) The effects of the Prandtl number on increasing dimensionless velocity components for a given system are investigated for Le = 1, N= M = 0.5 and Nb =Nt =Nr = 0.1. Fig. 4 (b) Impact of Prandtl number just on dimensionless temperature distribution for Le = 1, M =N= 0.5 and Nb =Nt =Nr = 0.1. Fig. 4 (c) The influence of the nanofluids profiles, Prandtl values just on dimensionless volume concentration of a nanofluids characteristics pictures have used a variety of applications Le = 1, M =N= 0.5 and Nb =Nt =Nr =0.1. The results of the comparison test are shown in table 2. Researchers have focused on the volume fraction of nanofluid profiles to determine the Prandtl number. It should be noticed that higher values of Pr result in decreasing values of $f(\eta)$.

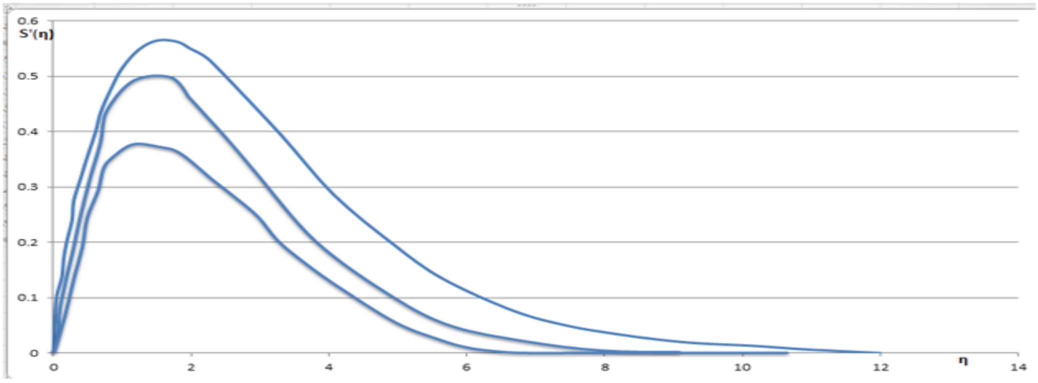

Fig. 4 (a). Impacts of the Prandtl number $s'(\eta)$.

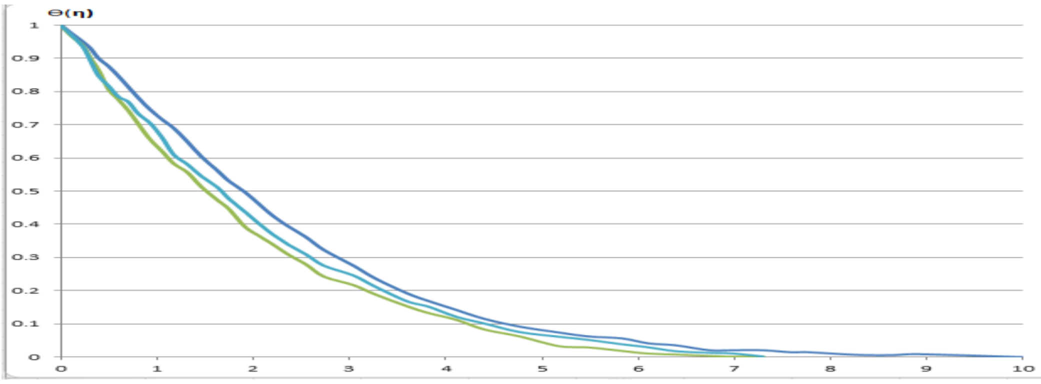

Fig. 4 (b). Impacts of the Prandtl number $\boldsymbol{\theta(\eta)}$.

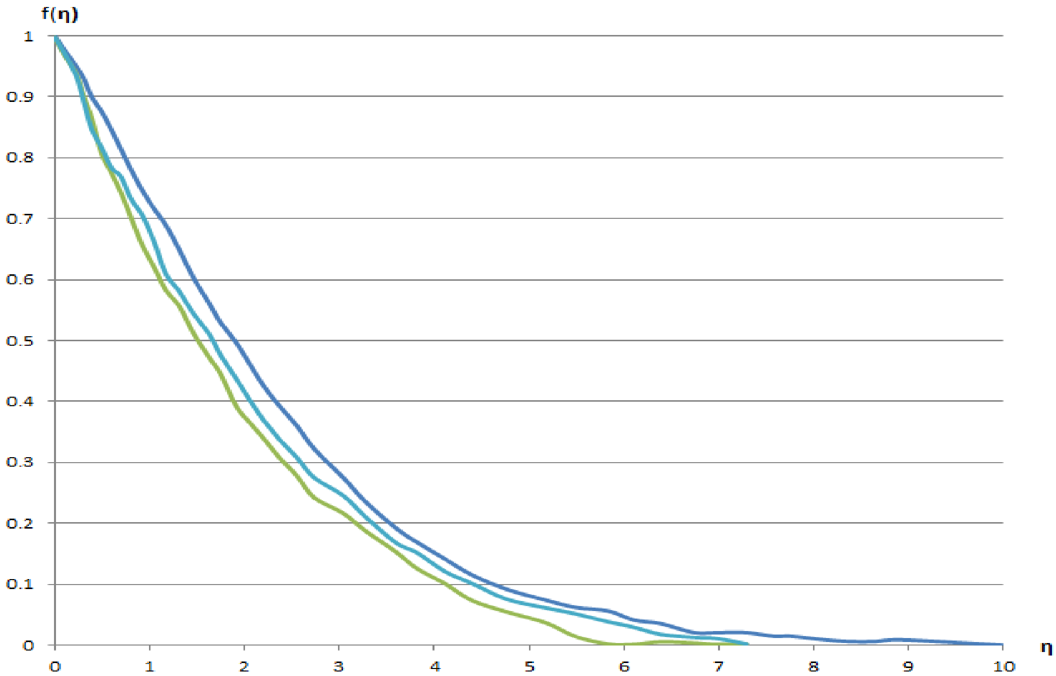

Fig. 4 (c). Impacts of the Prandtl number $f(\eta)$.

Nusselt number values that have been lowered $Nur = Rax^{\frac{1}{4}} Nu$ in the limit case of a constant fluid is defined as follows: The current findings are based on $Le = 10, Nr = Nb = Nt = 10^{-5}$.

Table 2

Comparison test results.

Pr	Bejan [12]	Present results
		Numerical
1	0.401	0.40102817
10	0.465	0.46496287
100	0.490	0.49000028

7. Result and discussion

Effects of magnetic fields or heat emission on a magnetic field incompressible viscous nano-fluid across a vertical plate have been investigated in the current study. Graphs illustrations for governing variables such as the Prandtl number are used to provide a clear understanding of the physical trouble results. As an exam of the precision of the current quantitative as well as analytical. A comparison is made between decreased Nusselt's morality and those reported by Nusselt inside the limiting circumstance of a frequent fluid. Table 2 shows that the comparison is favorable, as shown by the results. The dimensional velocity components rise as the value of Pr increases. This contrasts with a comparison that must be made with the Spontaneous convective of a standard fluid more than a vertical wall whereby the Prandtl number increases, the width of thehydraulic flow separation diminishes, and the vertical flow rate falls as the Prandtl numbers rise.

Unlike the traditional area of environment, The Prandtl current number used in the present study does not appear in the conservation of mass of advection on a vertical wall, whereas the Prandtl numbering used for the previous study does appear in the numerical solution, and as a result, its impact. The fluid velocity is significantly variable depending on the situation from the effect observed in traditional velocity profiles. Given that the Prandtl number reflects the relationship between dynamic viscosity and thermal diffusivity, it has been observed by scholars that higher Prandtl numbers are associated with thinner thermal boundary layers. The parameter known as the Prandtl number (Pr) governs the thickness of both momentum and thermal boundary layers, and it is influenced by the heat transfer equation.

The flow of a nanofluid sheet and the heat transfer division of an unsteady nanofluid flow into a stable nanofluid flow have been fully examined in the present work by using the Runge-Kutta method to solve nonlinear partial differential equations. Numerical solutions must be found for a variety of parameters that use the RK-4 order method. These include the Prandtl as well as Lewis number, the Brownian motions parameter, as well as the thermophoresis parameter.

The Runge Kutta technique Eq. (63)-(66) is used to solve the equations when the boundary conditions are applied to the nonlinear ordinary differential equations. Utilizing Von Karman's transformations,

$$`\eta = (\Omega/v_f)^{1/2} z, \quad u = \Omega r F(\eta), v = \Omega r G(\eta), w = (\Omega v_f)^{1/2} H(\eta) \tag{63}$$

$$\rho - \rho_\infty = 2_{\mu_f} \Omega_p(n), \theta(n) = (T - T_\infty)/(T_w - T_\infty) \tag{64}$$

$$H_1(\eta) = 2Ce^{-\eta}(-1 + e^\eta)h \tag{65}$$

$$F_1(\eta) = \frac{1}{6} e^{-3\eta}(-1 + e^\eta)h\left(-1 + C^2 - e^n + C^2 e^\eta - 3Ce^\eta \frac{1}{(1-\varphi)^{2.5}(1-\varphi+\varphi\rho_S/\rho_f}\right) \tag{66}$$

$$G_1(\eta) = \frac{1}{6} e^{-3\eta}(-1 + e^\eta)h\left(2C + 2Ce^\eta - 3e^\eta + C^2 e^\eta - 3Ce^\eta \frac{1}{(1-\varphi)^{2.5}(1-\varphi+\varphi\rho_S/\rho_f}\right) \tag{67}$$

$$\theta_1(\eta) = -\frac{e^{-2\eta}(-1+e^\eta)hk_{nf}/k_f}{2P_r(\rho c_\rho)_{nf}/((\rho c_\rho)_f} \tag{68}$$

In the above equation, all variable defines as follows: $\theta\eta$ represent the dimensionless temperature, P_r is a Prandtl number, and $(\rho c_\rho)_{nf}$ denote the heat capacity of nanofluid while $(\rho c_\rho)_f$ is denote Nanofluids have a high heat capacity. The relative density of nanoparticles is denoted by the letter C, v_f signifies the fluid kinematic viscosity, η is a similarity variable, ρ_∞ signifies the density at ambient fluid, ρ is density, T_w is the temperature of the stretching surface, T_∞ the temperature of the surrounding fluid is represented by t, whilst u and v represent the velocity profile along the x- and y-axes, respectively in the above equation. The impact of the nano-fluid profiles' dimensionless volume fraction on the non - dimensional volume concentration of the nanofluid profile's buoyancy ratio variable number is investigated for N = 0.5 , Pr = 1 and Nb = Nt = Nr = 0.1. Fig. 5 (a) shows a Lewis number influences dimensionless velocity components Prandtl for a variety of applications Nt=Nr=Nb 0.1. and Pr =1, N=M=0.5.

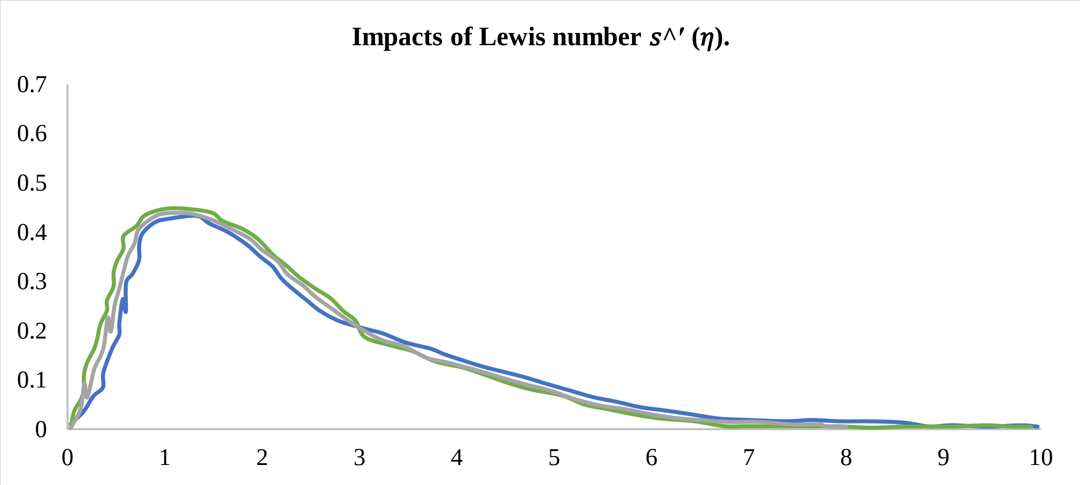

Fig. 5 (a). Impacts of Lewis number $s'(\eta)$.

For many purposes, the Lewis number only affects dimensionless velocity components. With Pr = 1 and Nb = Nt = Nr = 0.1, M = N = 0.5 shown in fig. 5 (b).

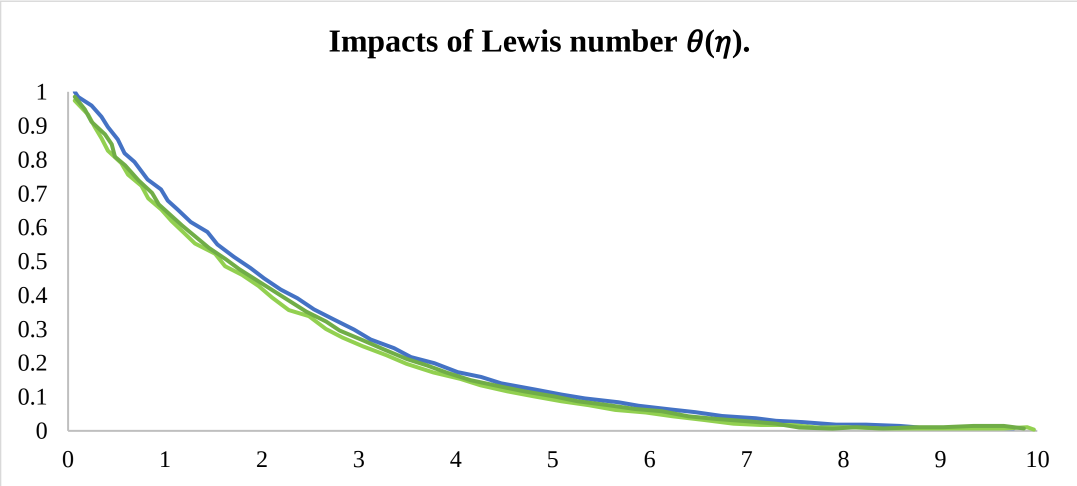

Fig. 5 (b). Impacts of Lewis number $\theta(\eta)$.

Fig. 5 (c) Reveal that an investigation has been conducted on the impact of the Lewis number alone on the dimensionless solid's capacity percentage of nanofluid profiles for Nb = Nt = Nr = 0.1 and Pr = 1, M = N = 0.5, while ensuring the absence of plagiarism.

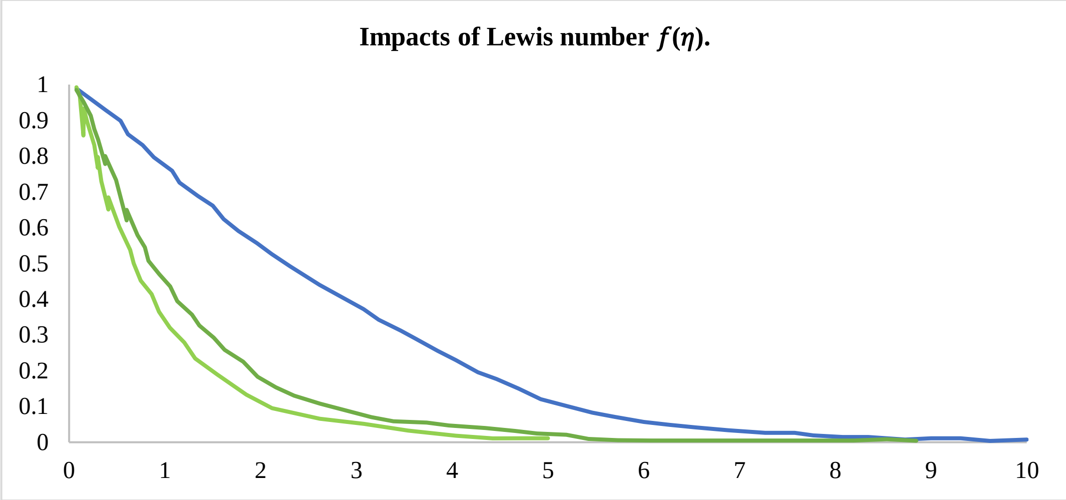

Fig. 5 (c). Impacts of Lewis number $f(\eta)$.

Extensive research was conducted to investigate the impact of multiple variables on dimensionless velocity, epidermis friction, temperatures, and heat transfer rate levels. Figure 6(a) displays the isolated influence of the magnetic parameter on non-dimensional velocity components for the spherical harmonic oscillator, specifically with Nb = Nt = Nr = 0.1, Pr = 1, Le = 1, and N = 0.5. The presence of a strong magnetic field in the boundary layer amplifies the Lorentz force, obstructing the flow in the opposite direction. Consequently, higher values of the magnetic parameter led to a decrease in the velocity of the nanofluid.

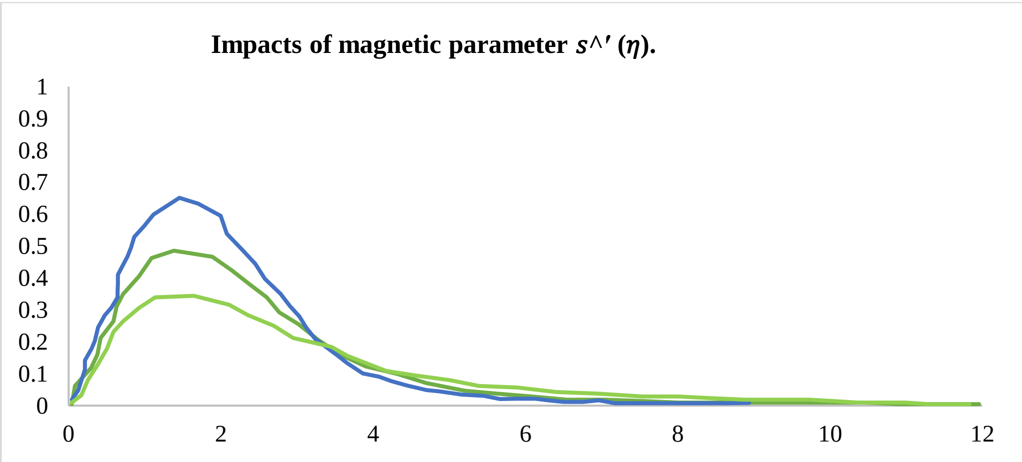

Fig. 6 (a). Impacts of magnetic parameter $s'(\eta)$.

When considering Nb = Nt = Nr = 0.1 and Pr = 1, Le = 1, N = 0.5, the impact of the magnetic parameter on two-dimensional temperature distributions is evident shown in fig. 6 (b).

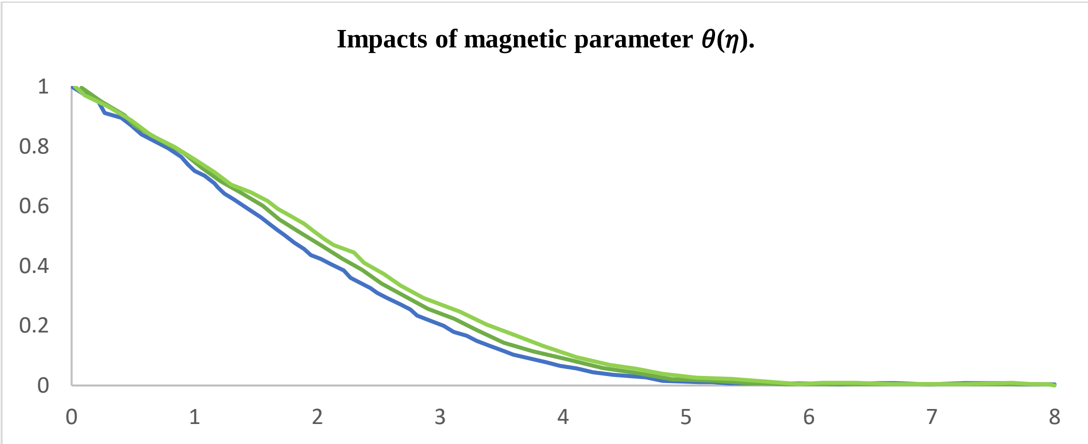

Fig. 6 (b). Impacts of magnetic parameter $\theta(\eta)$.

The effects of the magnetic parameter on the non-dimensional solid volume percentage of the nanofluid profiles were analyzed considering Pr = 1, Le = 1, N = 0.5, and Nb = Nt = Nr = 0.1 shown in fig. 6 (c).

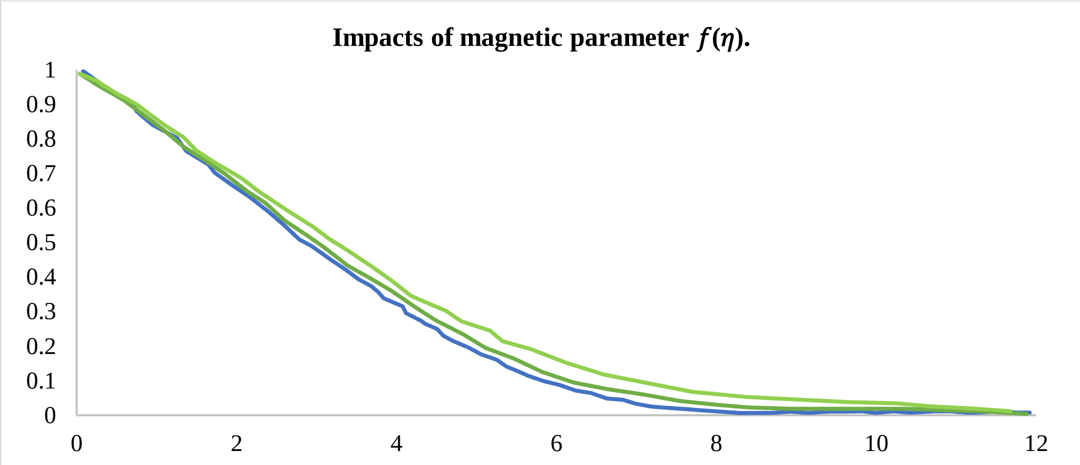

Fig. 6 (c). Impacts of magnetic parameter $f(\eta)$.

The effects of the radiation parameter on the two-dimensional velocity profile of the sphere of influence were analyzed for Nb = Nt = Nr = 0.1, Pr = 1, and N = 0.5, as depicted in Fig. 7(a).

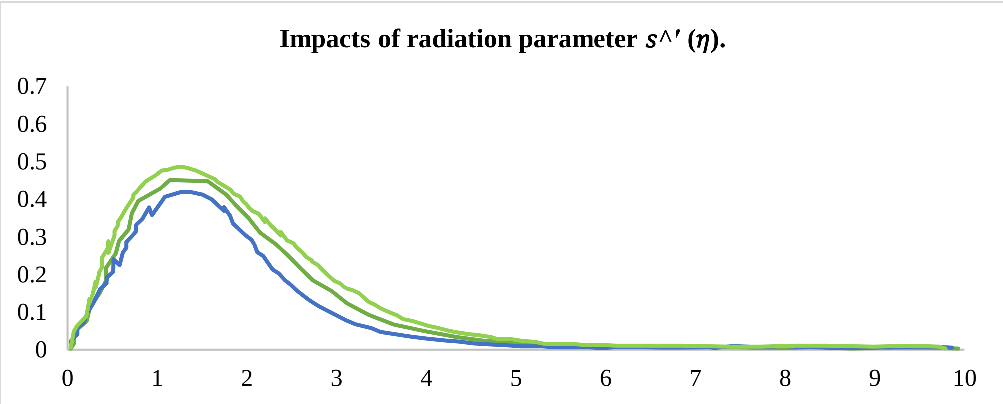

Fig. 7 (a). Impacts of radiation parameter $s'(\eta)$.

The experimental investigation focused on analyzing the influence of a radiation variable solely on the temperature profiles of various materials, under the conditions Nb = Nt = Nr = 0.1, Pr = 1, Le = 1, and N = 0.5 shown in fig. 7 (b).

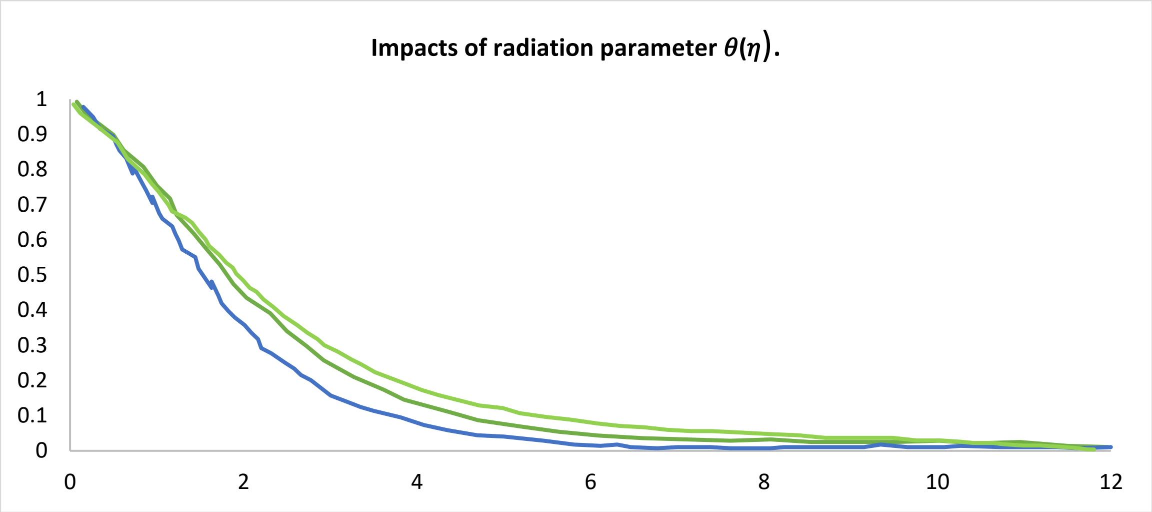

Fig. 7 (b). Impacts of radiation parameter $\theta(\eta)$.

Extensive research has been conducted to investigate the effects of varying the thermophoresis parameter number (Nb = Nt = Nr = 0.1 and Pr = 1, N = 0.5) on the dimensionless volume concentration of nanofluid profiles, considering a wide range of applications. shown in Fig. 7 (c).

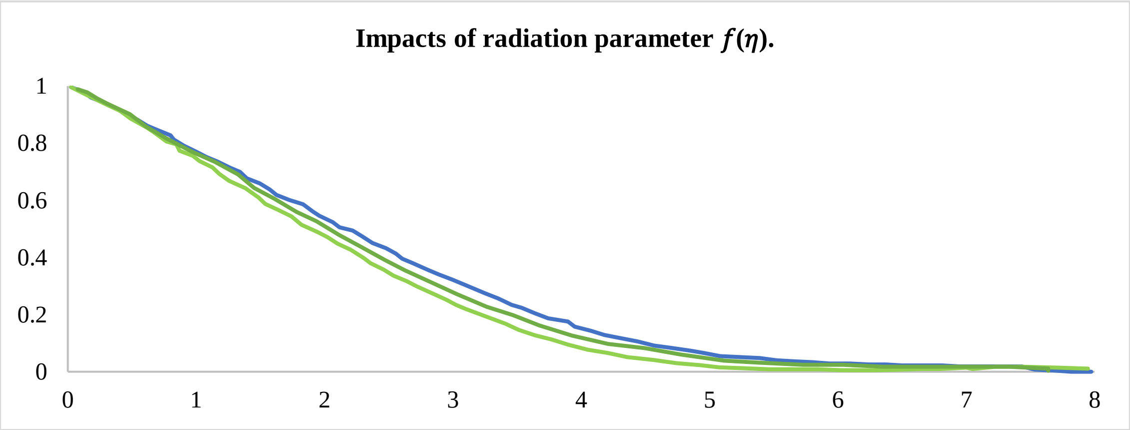

Fig. 7 (c). Impacts of radiation parameter $f(\eta)$.

Table 3 lists the values of the decreased Nusselt number (Nur) as well as the local Sherwood number (Shr) for various physical characteristics at different levels of resolution.

Table 3

With Nb =Nt = 0.3, the Variations of Nur and Shr

Le	**N**	**Nb**	**M**	**Nr**	**Pr**	**Nt**	**Shr**		**Nur**	
							Analytical	Numerical	Analytical	Numerical
10	1	0.3	1	0.3	5	0.3	0.241	0.2409	1.0324	1.0323
				0.4			0.2392	0.239	1.0196	1.0195
				0.5			0.2373	0.237	1.0061	1.006
10	1	0.3	1	0.3	5	0.3	0.241	0.2409	1.0323	1.0322
	2						0.2172	0.217	1.0598	1.059
	3						0.1992	0.199	1.0789	1.078
10	1	0.3	1	0.3	5	0.3	0.241	0.240	1.0323	1.032
					6		0.2455	0.245	1.0436	1.04355
					7		0.2492	0.249	1.053	1.0526
10	1	0.3	1	0.3	5	0.3	0.24	0.2411	1.0324	1.0323

11		0.241	0.240	1.0722	1.072
12		0.211	0.241	1.11	1.1096
	1	0.2409	0.241	1.03238	1.0323
	2	0.211	0.2109	0.95	0.947
	3	0.1899	0.189	0.885	0.884

There are theoretical and simulation conclusions to be drawn from this table a remarkable degree of consistency between the existing ones. As can be seen in Table 3, the Nur and Shr values follow the same general trends as Pr and Le, increasing with higher values, but decreasing with higher values of Nr and M. It seems that the thermal radiation factor has a significant impact on Nur and Shr. The rise in the radiation parameter results in a drop in the lowered Nusselt and a rise in the value of the local average Nusselt number as a result of the increased radiation parameter. For design and technology computations, this table gives data about the flow of heat transfer qualities and other relevant facts in a manner that is accessible to researchers and engineers. In this case, it is shown that both the radiation factor and the magnetization would have a significant impact on the heating operations in the nanofluid.

Fig. 8 (a) demonstrates that the effects of a buoyancy ratio variable on the one-dimensional velocity profile of acoustic waves are restricted to the values Nb=Nt=Nr 0.1 and Pr =1, M=N=0.5

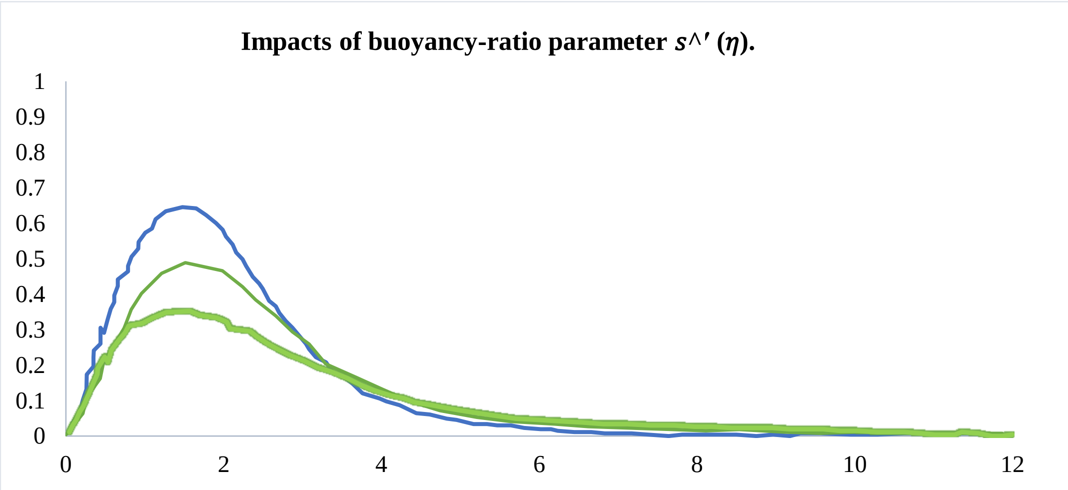

Fig. 8 (a) Impacts of buoyancy-ratio parameter $s'(\eta)$.

For a variety of materials, the Nb = Nt = Nr = 0.1 and Pr = 1, Le = 1, N = 0.5 buoyancy depth ratio has a significant effect on temperature distributions shown in fig. 8 (b).

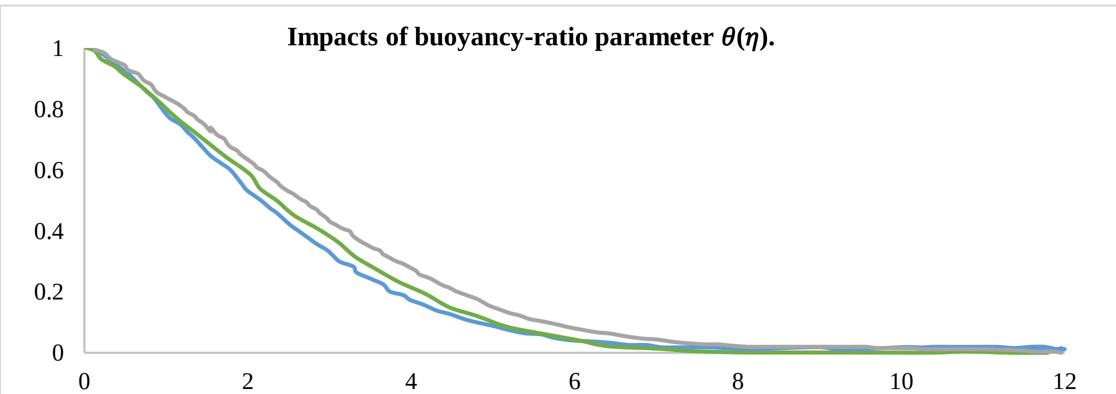

Fig. 8 (b) Impacts of buoyancy-ratio parameter $\theta(\eta)$.

Dimensionless solid volume percentage of nanofluid profiles as a function of buoyancy-ratio parameter for Nb =Nt =Nr = 0.1 and Pr = 1, Le = 1, M =N= 0.5Fig. 8 (c).

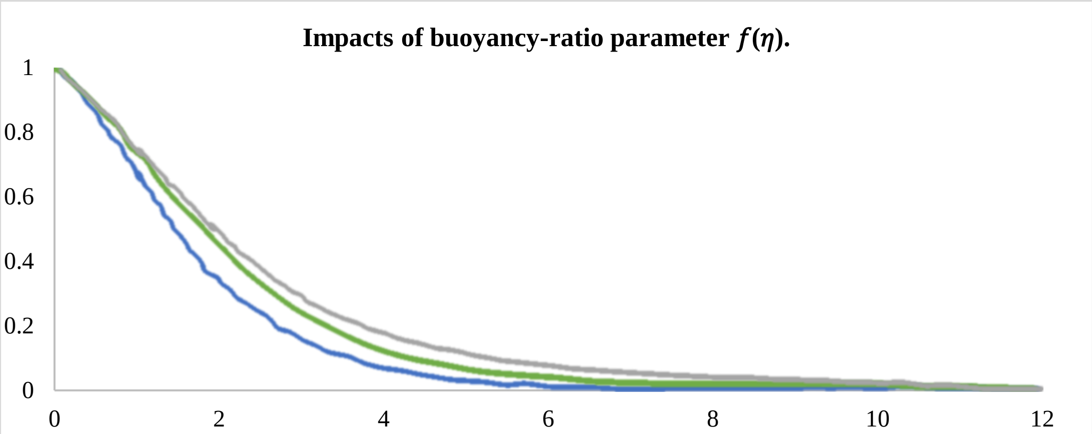

Fig. 8 (c) Impacts of buoyancy-ratio parameter $f(\eta)$.

Fig. 9 (a) demonstrates that in only one dimension Pr = 1, Le = 1, M = N = 0.5, and N b = N t = N r 0.1 does the Brownian motion parameter have any effect on the non-dimensional velocity profile of acoustic waves.

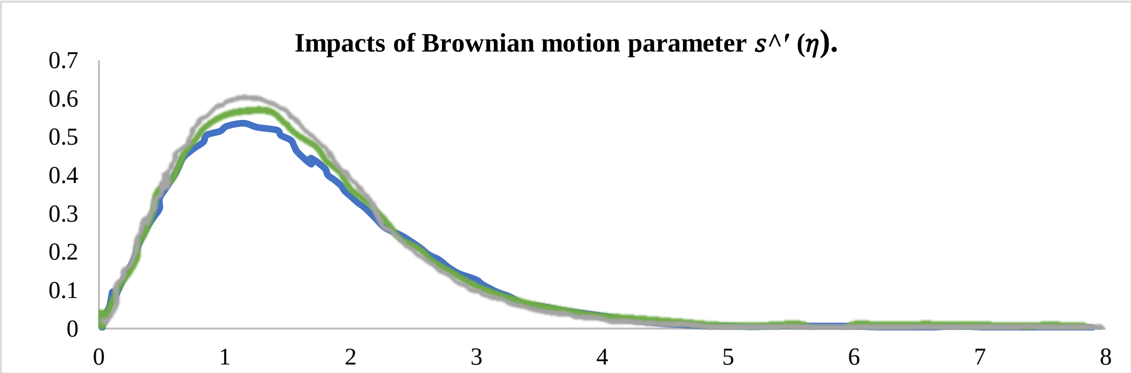

Fig. 9 (a) Impacts of Brownian motion parameter $s'(\eta)$.

Temperature distribution effects of the Brownian motion parameter ratio for Pr = 1, Le = 1, N = 0.5, and Nb = Nt = Nr = 0.1 for a variety of materials taken independently shown in Fig. 9 (b).

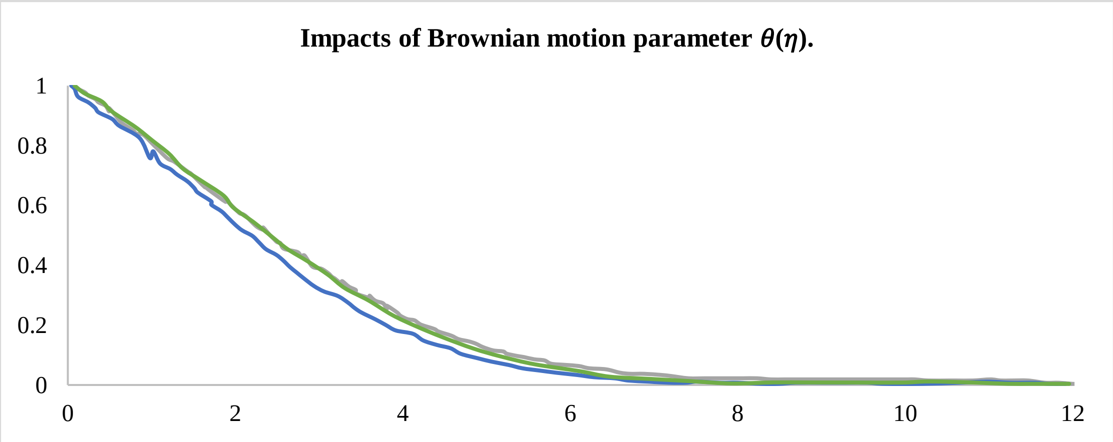

Fig. 9 (b) Impacts of Brownian motion parameter $\theta(\eta)$.

Dimensionless solid volume percentage in nanofluid profiles as a function of the buoyancy-ratio parameter for Nb =Nt =Nr = 0.1 and Pr = 1, Le = 1, M =N= 0.5. are shown in Fig. 9 (c).

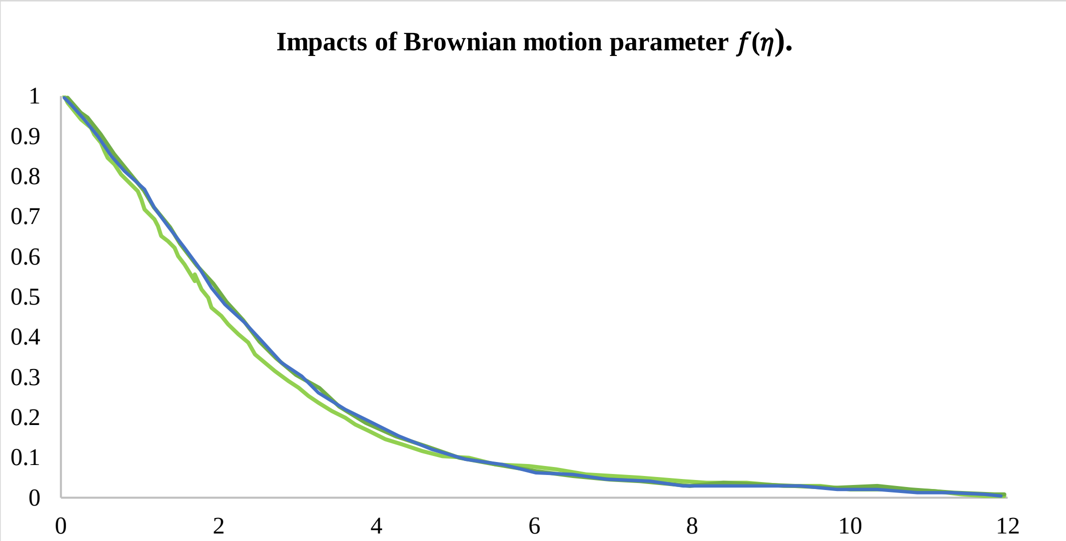

Fig. 9 (c) Impacts of Brownian motion parameter $f(\eta)$.

It is possible to acquire the equivalent mistake in that order. The constant nanofluid flow solution for t->∞ is obtained by utilizing steady boundary conditions, which are then observed by steady residual behavior. The numerical approach that was employed to solve the governing equations seems to be sufficiently robust and efficient for the suitable resolution of the class of issues under consideration. The observed local skin friction coefficient rises dramatically with increasing unsteadiness limitation but reducing the observed local skin friction coefficient causes a uniform decrease. The paper demonstrates that nanofluids are capable of significantly lowering the drag force generated by fluid movement. It is also important to note that the local Nusselt number grows in response to an increase in the unsteadiness parameter. Results showed that when the proportion of solids in the nanofluid grew, the Nusselt number increased as the skin friction factor decreased.

8. Conclusion and Future Work

A stretched rotating disc with 3 different kinds of nanoparticles (Cu, CuO, then Al2O3) is used to explore the flow and heat transmission of nanofluid. It has been shown that the differential transform approach must be effectively used to the solution of the presented problem. Nonlinear governing equations are transformed into ordinary differential equations via unstable equations, which are then explained using the Runge-Kutta method. The impacts of factors including the stretching strength parameter, the solid capacity percentage, and the kinds of nanofluids on speed and temperature fields are demonstrated and then investigated using numerical analyses. As the Pr, radiation factor, thermophoresis parameters and Brownian motion increase, so does the prominence of the velocity profile. Increases in the Prandtl number result in decreases in the temperature profile of the environment, whereas increases in all other parameters increase temperature distribution. As the value of the thermophoresis parameter rises, so do the nanofluidic flow profiles and the thermal rising pattern of the solid volume percentage. but the profile of radiation parameter value falls as the thermophoresis parameter value increases. The obtained solutions are in excellent accordance with RK-4, indicating that the proposed technique must be used to resolve different kinds of problems. The experimental outcome of the work shows that nanofluids may greatly reduce the drag force created by fluid flow. It is also important to note that increasing the unsteadiness parameter causes the local Nusselt number to increase. It was revealed that raising the solid volume percentage in the nanofluid lowered the local skin friction factor while increasing the local Nusselt number. If boundary layer nanofluid flow is to be developed in the future, it must be possible to solve the heat transfer equations using the Runge-Kutta method, which is a superior approach for solving differential equations numerically.

References

[1] Gugulethu, Srinu, and Vamsi Krishna Pasam. "Experimental investigation to study the performance of CNT/MoS2 hybrid nanofluid in turning of AISI 1040 step." Australian Journal of Mechanical Engineering (2020): 1-11. https://doi.org/10.1080/14484846.2020.1756067

[2] Chitsazan, Dariush, Amirfarhang Mehdizadeh, and Rouzbeh Riazi. "Heat transfer analysis of unsteady MHD rotating graphene oxide water nanofluid flow." Australian Journal of Mechanical Engineering 18, no. 2 (2020): 193-199. https://doi.org/10.1080/14484846.2018.1480099

[3] Ahmadi, A. R., A. Zahmatkesh, M. Hatami, and D. D. Ganji. "A comprehensive analysis of the flow and heat transfer for a nanofluid over an unsteady stretching flat plate." Powder Technology 258 (2014): 125-133. https://doi.org/10.1016/j.powtec.2014.03.021

[4] Yin, Chenguang, Liancun Zheng, Chaoli Zhang, and Xinxin Zhang. "Flow and heat transfer of nanofluids over a rotating disk with uniform stretching rate in the radial direction." Propulsion and Power Research 6, no. 1 (2017): 25-30. https://doi.org/10.1016/j.jppr.2017.01.004

[5] Noghrehabadi, Aminreza, Rashid Pourrajab, and Mohammad Ghalambaz. "Effect of partial slip boundary condition on the flow and heat transfer of nanofluids past stretching sheet prescribed constant wall temperature." International Journal of Thermal Sciences 54 (2012): 253-261. httips://doi: 10.1016/j.ijthermalsci.2011.11.017

[6] Daniel, Yahaya Shagaiya, Zainal Abdul Aziz, Zuhaila Ismail, and Faisal Salah. "Effects of slip and convective conditions on MHD flow of nanofluid over a porous nonlinear stretching/shrinking sheet." Australian Journal of Mechanical Engineering 16, no. 3 (2018): 213-229. https://doi.org/10.1080/14484846.2017.1358844

[7] Uddin, Ziya, Korimerla Sai Vishwak, and Souad Harmand. "Numerical duality of MHD stagnation point flow and heat transfer of nanofluid past a shrinking/stretching sheet: Metaheuristic approach." Chinese Journal of Physics 73 (2021): 442-461. https://doi.org/10.1016/j.cjph.2021.07.018

[8] Salari, Mahmoud, Mohammad Mohammadtabar, and Ali Mohammadtabar. "Numerical solutions to heat transfer of nanofluid flow over stretching sheet subjected to variations of nanoparticle volume fraction and wall temperature." Applied Mathematics and Mechanics 35, no. 1 (2014): 63-72. https://doi.org/10.1007/s10483-014-1772-8

[9] Thumma, Thirupathi, and Satya Narayana PV. "Innovations in Eyring–Powell radiative nanofluid flow due to nonlinear stretching sheet with convective heat and mass conditions: Numerical study." Australian Journal of Mechanical Engineering (2020): https://doi.org/10.1080/14484846.2020.1842158

[10] Daniel, Yahaya Shagaiya, Zainal Abdul Aziz, Zuhaila Ismail, and Faisal Salah. "Hydromagnetic slip flow of nanofluid with thermal stratification and convective heating." Australian Journal of Mechanical Engineering 18, no. 2 (2020): 147-155. https://doi.org/10.1080/14484846.2018.1432330

[11] Kumar, Anil, Sachin Sharma, Sunil Kumar, and Rajesh Maithani. "Thermohydraulic analysis of twisted tape inserts with SiO_2/H_2 O nanofluid in the heat exchanger." Australian Journal of Mechanical Engineering (2021): 1-14. https://doi.org/10.1080/14484846.2021.1960672

[12] LOGANATHAN, P., and S. SANGEETHA. "Natural Convection of Williamson Nanofluid Over a Semi-Infinite Vertical Plate in the Presence of Radiation." (2022). https://doi.org/10.21203/rs.3.rs-1877211/v1

[13] Siddique, Imran, Muhammad Nadeem, Jan Awrejcewicz, and Witold Pawłowski. "Soret and Dufour effects on unsteady MHD second-grade nanofluid flow across an exponentially stretching surface." Scientific Reports 12, no. 1 (2022): 1-14. https://doi.org/10.1038/s41598-022-16173-8

[14] Gugulethu, Srinu, and Vamsi Krishna Pasam. "Experimental investigation to study the performance of CNT/MoS2 hybrid nanofluid in turning of AISI 1040 step." Australian Journal of Mechanical Engineering (2020): 1-11. https://doi.org/10.1080/14484846.2020.1756067

[15] Chitsazan, Dariush, Amirfarhang Mehdizadeh, and Rouzbeh Riazi. "Heat transfer analysis of unsteady MHD rotating graphene oxide water nanofluid flow." Australian Journal of Mechanical Engineering 18, no. 2 (2020): 193-199. https://doi.org/10.1080/14484846.2018.1480099

[16] Ahmadi, A. R., A. Zahmatkesh, M. Hatami, and D. D. Ganji. "A comprehensive analysis of the flow and heat transfer for a nanofluid over an unsteady stretching flat plate." Powder Technology 258 (2014): 125-133. https://doi.org/10.1016/j.powtec.2014.03.021

[17] Yin, Chenguang, Liancun Zheng, Chaoli Zhang, and Xinxin Zhang. "Flow and heat transfer of nanofluids over a rotating disk with uniform stretching rate in the radial direction." Propulsion and Power Research 6, no. 1 (2017): 25-30. https://doi.org/10.1016/j.jppr.2017.01.004

[18] Noghrehabadi, Aminreza, Rashid Pourrajab, and Mohammad Ghalambaz. "Effect of partial slip boundary condition on the flow and heat transfer of nanofluids past stretching sheet prescribed constant wall temperature." International Journal of Thermal Sciences 54 (2012): 253-261. httips://doi: 10.1016/j.ijthermalsci.2011.11.017

[19] Daniel, Yahaya Shagaiya, Zainal Abdul Aziz, Zuhaila Ismail, and Faisal Salah. "Effects of slip and convective conditions on MHD flow of nanofluid over a porous nonlinear stretching/shrinking sheet." Australian Journal of Mechanical Engineering 16, no. 3 (2018): 213-229. https://doi.org/10.1080/14484846.2017.1358844

[20] Uddin, Ziya, Korimerla Sai Vishwak, and Souad Harmand. "Numerical duality of MHD stagnation point flow and heat transfer of nanofluid past a shrinking/stretching sheet: Metaheuristic approach." Chinese Journal of Physics 73 (2021): 442-461. https://doi.org/10.1016/j.cjph.2021.07.018

[21] Salari, Mahmoud, Mohammad Mohammadtabar, and Ali Mohammadtabar. "Numerical solutions to heat transfer of nanofluid flow over stretching sheet subjected to variations of nanoparticle volume fraction and wall temperature." Applied Mathematics and Mechanics 35, no. 1 (2014): 63-72. https://doi.org/10.1007/s10483-014-1772-8

[22] Thumma, Thirupathi, and Satya Narayana PV. "Innovations in Eyring–Powell radiative nanofluid flow due to nonlinear stretching sheet with convective heat and mass conditions: Numerical study." Australian Journal of Mechanical Engineering (2020): https://doi.org/10.1080/14484846.2020.1842158

[23] Daniel, Yahaya Shagaiya, Zainal Abdul Aziz, Zuhaila Ismail, and Faisal Salah. "Hydromagnetic slip flow of nanofluid with thermal stratification and convective heating." Australian Journal of Mechanical Engineering 18, no. 2 (2020): 147-155. https://doi.org/10.1080/14484846.2018.1432330

[24] Kumar, Anil, Sachin Sharma, Sunil Kumar, and Rajesh Maithani. "Thermohydraulic analysis of twisted tape inserts with SiO_2/H_2 O nanofluid in the heat exchanger." Australian Journal of Mechanical Engineering (2021): 1-14. https://doi.org/10.1080/14484846.2021.1960672

[25] LOGANATHAN, P., and S. SANGEETHA. "Natural Convection of Williamson Nanofluid Over a Semi-Infinite Vertical Plate in the Presence of Radiation." (2022). https://doi.org/10.21203/rs.3.rs-1877211/v1

[26] Siddique, Imran, Muhammad Nadeem, Jan Awrejcewicz, and Witold Pawłowski. "Soret and Dufour effects on unsteady MHD second-grade nanofluid flow across an exponentially stretching surface." Scientific Reports 12, no. 1 (2022): 1-14. https://doi.org/10.1038/s41598-022-16173-8